Controlling Morphology and Functions of Cardiac Organoids by Two-Dimensional Geometrical Templates

Plansky Hoang[1,2§], Shiyang Sun[1,2§], Bearett A. Tarris[1,2], Zhen Ma[1,2*]

1 Department of Biomedical and Chemical Engineering, Syracuse University

2 BioInspired Syracuse Institute for Material and Living Systems, Syracuse University

[§]These two authors equally contribute to this article.

Short Title: Geometry-Mediated Cardiac Organoid Engineering

*Corresponding Author

Zhen Ma, PhD.

Department of Biomedical and Chemical Engineering

Syracuse University

318 Bowne Hall

Syracuse, NY 13244, United States of America

Tel: (315) 443-4057

E-mail: zma112@syr.edu

Number of Tables: 0

Number of Figures: 3

Word Count: 3769

Keywords: Organoids, micropatterning, geometrical confinement, human induced pluripotent stem cells

Abstract

Traditionally, tissue-specific organoids are generated as 3D aggregates of stem cells embedded in Matrigel or hydrogels, and the aggregates eventually end up a spherical shape and suspended in the matrix. Lack of geometrical control of organoid formation makes these spherical organoids limited for modeling the tissues with complex shapes. To address this challenge, we developed a new method to generate 3D spatial-organized cardiac organoids from 2D micropatterned hiPSC colonies, instead of directly from 3D stem cell aggregates. This new approach opens the possibility to create cardiac organoids that are templated by 2D non-spherical geometries, which potentially provides us a deeper understanding of biophysical controls on developmental organogenesis. Here, we designed 2D geometrical templates with quadrilateral shapes and pentagram shapes that had same total area but different geometrical shapes. Using this templated substrate, we grew cardiac organoids from human induced pluripotent stem cells (hiPSCs) and collected a series of parameters to characterize morphological and functional properties of the cardiac organoids. In quadrilateral templates, we found that increasing the aspect ratio impaired cardiac tissue 3D self-assembly, but the elongated geometry improved the cardiac contractile functions. However, in pentagram templates, cardiac organoid structure and function were optimized with a specific geometry of an ideal star shape. This study will shed a light on "*organogenesis-by-design*" by increasing the intricacy of starting templates from external geometrical cues to improve the organoid morphogenesis and functionality.

Introduction

Organoid technology offers us a unique opportunity to recapitulate the biological process of organogenesis into spatially organized tissue structures, which resemble the architecture and functionality of specific tissues[Yin et al., 2016; Brassard, and Lutolf, 2019; Hofer, and Lutolf, 2021]. Organ development is directed by surrounding biochemical signals and biophysical cues in utero[Nelson, and Gleghorn, 2012]. 3D organoid technology built upon fundamental concepts of developmental biology relies on dynamic multicellular self-organization to form functional biological tissues under the control of extracellular microenvironment. Conventional differentiation from hiPSCs and human embryonic stem cells (hESCs) were primarily conducted under 2D cell culture systems. Although this method is suitable for day-to-day hiPSC culture expansion, differentiated tissues on standard tissue culture surfaces ultimately lack region-specific structure and architecture seen in native tissues[McKee, and Chaudhry, 2017; Hofer, and Lutolf, 2021]. Monolayer hiPSC differentiation, therefore, does not accurately represent the complexity of morphogenetic events during organogenesis[Kim et al., 2020], which are governed by the synergistic interactions of biochemical and biophysical factors. Therefore, there is a critical need to understand the role of biophysical constraint on key metrics of organ development, including growth, differentiation, and cellular and tissue function.

Cell patterning methods have been used extensively to study the biological behaviors and functions of stem cells by creating specific geometrical constraints. Extensive efforts based on surface patterning techniques are carried out in the stem cell field in order to understand the synergy between intrinsic and extrinsic factors involved in cell fate specification, patterning, and symmetry[Tang et al., 2010; Wan et al., 2011; Kolind et al., 2012]. The patterned surfaces allow for control over cell-surface interactions and create biophysical gradients that affect the cell size, morphology and differentiation. Early studies on micropatterning mesenchymal stem cells (MSCs) showed that stem cell differentiation can be driven by the geometrical constraints that altered cytoskeletal tension[Kilian et al., 2010]. This work, and many more[Zhang et al., 2013; Shukla et al., 2016; Loye et al., 2018; Yang et al., 2018], illustrated that specific geometrical features promoted actomyosin remodeling and contractility on the modulation of osteogenesis and adipogenesis of MSCs. Taking into the consideration of intercellular interactions, micropattern designs were changed to increase the total cell number per pattern from one to nine cells, which demonstrated an enhancement of osteogenic activity with the increasing cell numbers. Overall, these early 2D studies highlighted the crucial role of geometrical cues on controlling stem cell differentiation via mechanotransduction-dependent pathways.

Furthermore, 2D surface patterning has been applied to study early embryogenesis using pluripotent stem cells, such as germ layer patterning[Deglincerti et al., 2016; Simunovic, and Brivanlou, 2017; Morgani et al., 2018; Britton et al., 2021]. With the treatment of developmental growth factors, the hESCs under patterned geometrical confinement formed self-organized differentiation with specific radial domains. Each domain expressed the markers associated with one specific germ layer, which recapitulated the early gastrulation. These studies also showed that the cell patterning outcome was dependent on the micropattern geometry size, indicating a correlation between fate specification and 2D geometrical templates. In the context of organoid engineering, kidney organoids generated by micropatterning techniques were used to model tubulogenesis process in vitro[Bosch-Fortea et al., 2019], demonstrating comparable physiological formation of a vascular lumen surrounded by renal epithelium. More recent work based on hESC micropatterning generated the neural organoids, called neuruloids, for the modeling of neurulation[Haremaki et al., 2019]. Neural induction of micropatterned hESCs accelerated the formation of neural rosettes, which is a key feature of neural progenitor development. As a disease model, neuruloids with the Huntington's disease mutations showed early defects within the neural rosettes, such as loss of radial symmetry and reduction in lumen size. Given the difficulty of studying brain developmental disorders in humans, this system serves as a promising alternative to characterize human ectodermal development and identify morphological factors involved in developmental neural diseases. These examples illustrate the critical need for spatiotemporal guidance via cell microenvironments to guide the structure and function of stem cell organoids of specific biological tissues.

Previous work from our lab discussed how micropattern geometry influences the architecture of cardiac organoids generated from simple shape designs of circular patterns with different geometrical sizes[Hoang et al., 2021]. In this work we varied the complexity of 2D geometrical templates with the same geometrical area but different

quadrilateral and pentagram shapes, which altered the biophysical constraint gradients within each shape. We found that factors, such as aspect ratio (quadrilateral) and central area (pentagram) influence organoid self-assembly and cardiac functions because of the changes in cellular distribution and cell-edge contact. The geometries chosen in this study highlighted the influence of biomechanical cues on cardiac differentiation and tissue assembly. Each geometry presented the variations in cellular localization within patterned cell colonies, specifically cell-edge contact with the pattern perimeters in the pentagram geometries. In addition to biomechanical variations, rectangular shapes also presented potential biological relevance, as they can be used to model linear heart tube formation during early embryogenesis. This allowed us to study how the changes in biophysical cues from these complex geometrical templates drove the development of cardiac organoids to their tissue architectures and functions.

Materials and Methods

Micropatterning of tissue culture surfaces

Surface micropatterning on tissue culture polystyrene was carried out using the selective etching approach described previously [cite]. Poly(dimethyl siloxane) (PDMS) was casted from SU8 masters with designed features to produce thin elastomeric stencils with clear-through holes. Non-fouling poly(ethylene glycol) (PEG) solution was grafted onto 6-well tissue culture plates and cured under UV light exposure (Dymax UV Illuminator; model no. 2000EC). Micropatterns were fabricated by selective oxygen plasma etching (Oxygen plasma treatment system, PlasmaEtch PE50XL) of the PEG layer using the PDMS stencils. Micropatterned tissue culture plates were sterilized by immersing in 70% ethanol for 1 hour and subsequent washing with sterile phosphate buffered saline (PBS).

Generation of cardiac organoids

Micropatterned surfaces were coated with diluted Geltrex hESC-qualified matrix (Life Technologies, cat. no. A1413302) and seeded with GCaMP6f hiPSCs in Essential 8 (E8) medium (Life Technologies, cat. no. A1517001). Cardiac differentiation was initiated (Day 0) when the micropatterns reached confluency, and performed via small molecules[Lian et al., 2013; Lian et al., 2012] of GSK3 inhibitor CHIR99021 (Day 0) (Stem Cell Technologies, cat. no. 72054) and WNT pathway inhibitor IWP4 (Day 2) (Stem Cell Technologies, cat. no. 72554) in RPMI 1640 medium (Life Technologies, cat. no. 11875093) supplemented with B27-minus insulin (RPMI/B27 minus insulin) (Life technologies, cat. no. A1895601). At Day 6 onward, organoids were maintained in RPMI 1640 medium supplemented with complete B27 supplement (RPMI/B27 Complete) (Life Technologies cat. no. 17504044) until Day 20 for contractile and structural analysis.

Immunofluorescence staining and morphological characterization

Organoids were characterized based on immunofluorescence staining of cardiac tissue with cardiac troponin T (cTnT) and entire organoid structure with actin (Phalloidin). Samples were fixed with 4% (vol/vol) paraformaldehyde (PFA) for 10 minutes, permeabilized with 0.2% (vol/vol) Triton X-100 and blocked with 2% (wt/vol) bovine serum albumin (BSA). Samples were incubated with primary antibody against cTnT (dilution 1:200) for 1 hour and then incubated with secondary antibody, together with Phalloidin for 1 hour at room temperature. Leica Thunder upright fluorescent microscope with a 40X water immersion objective was used to capture z-stacks of the organoids for height measurements and Z-projection in ImageJ. The *Area Ratio* was measured by using the circular or elliptical tool to approximate the area of fluorescence of GCaMP flux for cardiac tissue and normalizing this area relative to the area of the entire pattern. The *Height* was measured by locating the top and bottom of the organoids.

Functional characterization of cardiac organoids

GCaMP6f hiPSC-derived cardiac organoids were imaged in an onstage microscope incubator (OkoLab Stage Top Incubator, UNO-T-H-CO2) at 37 ˚C and 5% CO2 to maintain standard physiological conditions on a Nikon Ti-E inverted microscope with Andor Zyla 4.2+ digital CMOS camera. Videos of contracting cardiac organoids were recorded at 50 frames per second for ten seconds in brightfield and exported as a series of single frame image files. Contraction physiology was assessed using video-based motion tracking software that computes motion vectors based on pixel movement. The motion vectors were assimilated into a contraction motion waveform representative of contractile physiology. Contraction physiology was also assessed by recording the calcium transient of organoids.

Videos were taken under 488 nm excitation at 40 milli-seconds exposure time with 25 frames per second. Calcium flux signals were exported as Z-axis profiles in ImageJ. The fluorescence bleaching decay was corrected and related parameters $\tau_0, \tau_{50}, \tau_{75}$ were computed using in-house MATLAB scripts. The time interval τ_0 is defined as the time it takes for the calcium flux to reach peak fluorescence intensity, whereas τ_{50} and τ_{75} represent the time it takes for the calcium flux to decay 50% and 75% of the peak fluorescence, respectively.

Statistical Analysis

Data was plotted as box plots. For single comparisons between two individual groups, a two-sided Student's t-test was used, and $p \leq 0.05$ was considered significant. For comparisons between more than two groups, one-way analysis of variance (ANOVA) was performed and $p \leq 0.05$ was considered significant. ANOVA analysis was supplemented with Tukey's multiple comparison test to determine significance between groups.

Results

Quadrilateral and pentagram ratios influence cardiac organoid structure

In this work, we generated cardiac organoids using PEG surface micropatterning as described by Hoang et al 2018. Geometrical templates of quadrilateral and pentagram geometries were designed using computer aided design software and translated onto photomasks for photolithography and soft lithography processing. Quadrilateral geometries were varied based on rectangular aspect ratio from 1:1 (R1), 1:2 (R2), 1:3 (R3), and 1:4 (R4), while keeping the template area constant across all geometries (Fig. 1a). The pentagram templates were designed by varying the center pentagon area and adjusting the area of the triangular vertices such that the area across all four pentagram designs were constant. Pentagram 1 (P1) was designed to have the smallest center pentagon area with the longest and sharpest triangular vertices, while Pentagram 4 (P4) had the largest center pentagon area with the shortest and bluntest vertices (Fig. 1b). This allowed us to investigate the influence of the biophysical stress of the pentagram points on cardiac organoid formation and function.

Immunofluorescence staining was used to visualize the distribution of cardiac muscle across the organoids and reconstruct the 3D images to characterize the tissue morphology (Fig. 1c, d). For quadrilateral organoids, there was a significant decrease in tissue height as the rectangular aspect ratio increased (Fig. 1e). This suggested that rectangular templates with larger aspect ratios is less favorable for cellular self-assembly into 3D tissues during differentiation. At the initial cell distribution, there is a lower degree of uniform radial distribution in 1:4 template, relative to 1:1 square template, which limited the areas where the cells can assemble into a larger organoid. Organoids cultured on pentagram geometries also showed the dependence of organoid formation on the template geometry (Fig. 1f). P1 organoids with the smallest center pentagon area had the smallest height and 3D architecture. Relative to the P1 template, as the pentagon center area increased, there was an improvement in the tissue height with P2-4 templates. However, the height was significantly greater only for the cardiac organoids generated from the P2 templates, suggesting that this geometry achieved the optimal tissue assembly. The pentagram with higher and more sharp-cornered geometries, such as P1 template, limited uniform radial cell distribution and subsequently reduced the tissue formation. This suggests that by varying the geometrical templates on 2D surface, organoid structure can be fine-tuned to precisely direct the tissue morphogenesis.

Cardiac functional outputs are dependent on the template geometries

To characterize the contraction physiology, we used an integrated assessment of the GCaMP6f calcium flux and cardiac contraction motion (Fig. 2a-d, Supplemental Movies 1-8). As we increased the rectangular aspect ratio, the beat rate was significantly decreased in R3 and R4 templates (Fig. 2e), which was also correlated with a significant increase of the area ratio (Fig. 2f) between contracting tissues and template area. We also saw that larger aspect ratio rectangular templates resulted in higher maximum calcium flux (Fig. 2g), which also took less time to reach peak fluorescence as indicated by a decreased τ_0 (Fig. 2h) for the R3 and R4 templates. This showed that increasing aspect ratio improved the muscle calcium release properties. However, across different quadrilateral templated cardiac organoids, the calcium decay properties, τ_{50} (Fig. 2i) and τ_{75} (Fig. 2j), showed no significant differences, indicating negligible effect of aspect ratio on calcium reuptake. In addition, we found that square templated organoids had significantly lower contraction (Fig. 2k) and relaxation velocities (Fig. 2l), in comparison to the

organoids from rectangular templates. We believe that rectangular templates allowed a certain level of alignment of cardiac tissues, which has been approved to improve contractile functions *in vitro*.

Pentagram templates (Fig. 3a-d, Supplemental Movies 9-16) were all able to form contracting cardiac tissue, primarily localized to the center. As we increased the center area, the beat rate (Fig. 3e) showed a slight decrease, but only was significantly lower in P3 templates. We found that P1 templates produced the cardiac organoids with higher area ratio (Fig. 3f) but lowest height, indicating that this design only generated a shallow layer of cardiac muscle that had greater distribution across the template, rather than a dome-like tissue structure at the template center as the other templated organoids. This also suggested that the organoid self-assembly into a pronounced architecture requires a 2D template with a large enough center portion to support 3D tissue formation. Regarding calcium handling properties, calcium transients remained relatively consistent, but with only P3 templates having significant deviations (Fig. 3g-j). As we increased the center area, we saw a reduction in contraction motion (Fig. 3k, l), especially comparing P1 and P2 versus P3 and P4 templates. However, we saw a peak in the values of contraction and relaxation velocities at P2 template, which was correlated with the trend of morphological measurements of height and area ratio for P2. This suggests that P2, which is an ideal star polygon, was the optimal shape to achieve the largest range of contractile motion, as well as the most robust cardiac tissue distribution and architecture.

Discussion

Stem cell-derived organoids are designed to resemble the early developing organs through self-organization of differentiating cells into spatially distinct tissue-specific structures. Although organoid models have been optimized for many major organs, such as intestine and liver, cardiovascular organoid development is still insubstantial. Recent work in cardiac organoids, however, have demonstrated great success in recapitulating key morphogenetic events in heart development, such as chamber formation and appropriate lineage specification. Moreover, many of these developments take advantage of temporal regulation of WNT signaling for the elucidation of heart development[Hellwarth et al., 2021]. Heart-forming organoids were developed using a well-established organoid culture system by embedding hPSC aggregates in Matrigel and differentiating with small molecules for canonical WNT pathway modulation[Drakhlis et al., 2021]. These cardiac organoids showed distinct spatial organization of myocardial, endocardial, and septum-transversum-like tissue layers. In addition to heart-related tissue types, these organoids also possessed endoderm and vascular phenotypes, illustrating the early co-development of mesoderm and endoderm tissues. Recent work developed human cardiac organoids by aggregating PSCs in low attachment 96-well plates and differentiating into human heart organoids (hHOs) using BMP4, Wnt-C59, and Activin-A mediated cardiac differentiation. These organoids began to contract as early as Day 6 of differentiation and can be maintained beating over 8 weeks. Through transcriptomic profiling, this work highlighted that these cardiac organoids closely modelled human fetal cardiac development and presented all main cardiac lineages[Lewis-Israeli et al., 2021]. To model the cardiac chamber formation *in vitro*, cardioids intrinsically produced chamber-like cavities through synergistic WNT and BMP activity that influenced the HAND1 signaling pathways[Hofbauer et al., 2021]. In the context of recapitulating morphological and structural aspects of the developing heart, murine heart organoids were developed by differentiating embryonic bodies (EBs) in the presence of FGF4, which promoted chamber formation and ECM production. The resulting organoid possessed atrium and ventricle-like structures, as well as smooth muscle and endothelium, which were structurally similar to the embryonic hearts[Lee et al., 2020]. These cardiac organoid models offer powerful tools to study mechanisms of cardiac lineage specification and structural morphogenesis. In comparison to direct 3D aggregation presented by these works, our cardiac organoids were generated from 2D micropatterned hiPSC colonies, allowing for cell self-organization into 3D tissue structures under geometrical confinement. Our approach opens the possibility and versatility to precisely engineer organoids under pre-designed templates, which could possibly resemble the similarity to developmental-inspired tissue shapes, such as linear heart tube fusion and looping events.

2D cell micropatterning offers a versatile way to define the cell number and the tissue geometry and modify the boundary conditions that cells can sense and self-organize, which has allowed us to engineer organoids with controlled tissue morphogenesis processes. These phenomena have been exemplified in the works modeling early

gastrulation, where hESCs were confined and underwent self-patterning into radial domains that resembled early germ layer emergence[Warmflash et al., 2014; Deglincerti et al., 2016; Simunovic, and Brivanlou, 2017]. A recent study of gastruloids showed radial expression gradient of mesoderm, endoderm, and ectoderm markers in micropatterned hPSC differentiation. Single-cell RNA sequencing results unveiled that additional cell types also emerged within this gastruloid system, including epiblast, trophectoderm, and primordial germ cells. Furthermore, by comparing with mouse and primate embryos, the transcriptomic profile confirmed that these engineered gastruloids recapitulated the primate-specific features of embryogenesis[Minn et al., 2020; Minn et al., 2021]. These gastruloids resembling the spatial tissue development during early embryogenesis pose the question of why cell position has such a strong influence on pattern formations. Therefore, it is imperative to understand how embryonic patterning is mediated through a series of paracrine signaling resulted from differential morphogen secretions across micropatterned cell colonies.

To examine the role of BMP signaling in gastruloid formation, it was found that differentiation was more sensitive and homogeneous in confined colonies with a controlled cell number. The geometrical confinement optimized the interactions between cell neighbors that led to sustained signaling not only for pluripotency maintenance, but also for efficient germ layer specification. This phenomenon referred to "*community effect*", meaning that cellular communication could maintain a state for a collection of cells to respond the external morphogens with high precision[Nemashkalo et al., 2017]. Moreover, this micropatterning experimental system was integrated with reaction-diffusion-based computational modeling to understand the correlation between small molecule induction and positional information on gastrulation-like patterning. This integrated model system illustrated that the radial germ layer organization in micropattern-mediated gastruloid development was mediated by spatial diffusive gradient of BMP4 and SMAD activity[Tewary et al., 2017]. Using this integrated model system, it is possible to predict how micropattern geometry influences fate patterning for more precise gastruloid engineering. The micropatterning-based system was also used to model the formation of the primitive streak based on WNT modulation[Martyn et al., 2019]. Cells at the micropattern perimeter highly expressed E-cadherin, which is an antagonist of WNT signaling. This indicated that biophysical constraint at the pattern perimeter retained E-cadherin expression and inhibited WNT activity on the hPSCs. As a result, WNT activation was temporally localized at the pattern centers leading to a spatial tissue patterning during primitive streak formation. These works stress the importance of precise engineering of organoid microenvironments to guide self-organization through the control of colony geometry, and how the microenvironment can offer spatiotemporal control of differentiation. Therefore, it would be of great interest for future work to investigate how spatial confinement controls signaling events that dictate the synergy of developmental patterning, tissue morphogenesis and tissue function of cardiac organoids.

Though this study did not focus on the molecular signaling mechanisms that drive the spatial tissue morphogenesis, we believe that several signaling pathways, including RhoA/ROCK and YAP/TAZ, might be involved in our findings. Our previous work demonstrated that small pattern sizes induced higher mechanical stress to the cells at the perimeter and consequently promoted higher RhoA/ROCK activity[Ma et al., 2015]. Similarly, we expect that geometries with a greater ratio of cells at the perimeter also have greater activation of RhoA/ROCK-related signaling transduction. For example, YAP/TAZ has been considered as a key downstream signaling from RhoA/ROCK pathway to cascade the signals to the nuclei. YAP/TAZ activity has been recognized as one of the key mechanotransducers that respond to cell polarity, surface area, and cell density[Virdi, and Pethe, 2021; Dupont et al., 2011; Aragona et al., 2013]. Specifically in cardiac differentiation, increased YAP activity was also linked to the enhancement of cardiomyocyte differentiation and promotion of cardiac tissue maturation[Heng et al., 2020; Mills et al., 2017]. Here, we infer that the different geometrical shapes used in this study might vary the degree of YAP/TAZ signaling activity. At early differentiation stages of our cardiac organoids, we showed that micropatterned substrate could influence cell shape depending on the location of individual cells within the patterns[Ma et al., 2015]. Cells along the perimeter had elongated and polarized morphologies, whereas cells at the center were more rounded. Other studies have shown that cells with rounded morphology had reduced cell adhesion and further reduced YAP/TAZ activity, which might create a morphogen gradient across the patterned cell colonies[Loye et al., 2018].

Most research on stem cell organoids generated under geometrical templates focused primarily on tissue pattern formation, but lack of investigation on the correlations between template geometries and tissue phenotypes. In this work, we explored how varying the geometrical template can influence cardiac organoid development and cardiac functional properties using quadrilateral and pentagram designs, which were easily modified to change the degrees of cell-edge contact and cell distribution. We observed that change of the area-to-perimeter ratios by different geometrical templates had a significant effect on both 3D morphology and contractile functions of the cardiac organoid. In particular, with pentagram geometries, P2 had the most optimal structure and function metrics. In our previous work[Hoang et al., 2021], circular geometries with increasing size also showed an optimal structure and function metrics at 600 μm diameter. We believe that a similar trend occurred in the pentagram shapes with radial symmetry, as the center pentagon area varied. Furthermore, our results showed that template geometry can significantly alter cardiac function, giving the ability to establish rationale design for organoid engineering with predictable structure-function correlation. Based on these results, we can conclude that microenvironment is critical for stem cell differentiation and organoid formation, as these biophysical interactions create necessary gradient of biochemical signaling essential for tissue spatial patterning. In future, we believe this study can be further strengthened with deep molecular biology analysis of signaling pathways that are associated with cell differentiation and tissue morphogenesis at different developmental timepoints. Furthermore, we can also incorporate high resolution imaging techniques to closely examine how cardiac myofibril structures, such as sarcomeres, can be modulated by different geometrical templates. These additional studies can supplement and shed light on why organoid architecture and cardiac output is favored under certain geometries.

Statement of Ethics

No animal or human subjects were used in this study and ethics approval was not required to conduct this work.

Conflict of Interest

The authors declare no competing interests.

Funding Sources

This work was supported by the NIH NICHD [R01HD101130] and NSF [CBET-1804875, CBET-1943798 and CMMI-2130192].

Author Contributions

P.H., S.S. and Z.M. conceived the study. S.S. performed all experiments and collected raw data. B.T. processed and analyzed recorded video. P.H. analyzed and interpreted data. P.H. and Z.M. wrote the manuscript.

Data Availability

All relevant raw data used to support the findings of this paper are available in the Supplementary Materials and upon request. Requests should be addressed to Z.M.

References

Aragona M, Panciera T, Manfrin A, Giulitti S, Michielin F, Elvassore N, et al.: A mechanical checkpoint controls multicellular growth through YAP/TAZ regulation by actin-processing factors. Cell 2013;154:1047–1059.

Bosch-Fortea M, Rodriguez-Fraticelli AE, Herranz G, Hachimi M, Barea MD, Young J, et al.: Micropattern-based platform as a physiologically relevant model to study epithelial morphogenesis and nephrotoxicity. Biomaterials 2019;218. DOI: 10.1016/j.biomaterials.2019.119339

Brassard JA, Lutolf MP: Engineering Stem Cell Self-organization to Build Better Organoids. Cell Stem Cell 2019;24:860–876.

Britton G, Chhabra S, Massey J, Warmflash A: Fate-Patterning of 2D Gastruloids and Ectodermal Colonies Using Micropatterned Human Pluripotent Stem Cells. Methods Mol Biol 2021;2258:119–130.

Deglincerti A, Etoc F, Guerra MC, Martyn I, Metzger J, Ruzo A, et al.: Self-organization of human embryonic stem cells on micropatterns. Nat Protoc 2016;11:2223–2232.

Drakhlis L, Biswanath S, Farr CM, Lupanow V, Teske J, Ritzenhoff K, et al.: Human heart-forming organoids recapitulate early heart and foregut development. Nat Biotechnol 2021;39:737–746.

Dupont S, Morsut L, Aragona M, Enzo E, Giulitti S, Cordenonsi M, et al.: Role of YAP/TAZ in mechanotransduction. Nature 2011;474:179–184.

Haremaki T, Metzger JJ, Rito T, Ozair MZ, Etoc F, Brivanlou AH: Self-organizing neuruloids model developmental aspects of Huntington's disease in the ectodermal compartment. Nat Biotechnol 2019;37:1198–1208.

Hellwarth PB, Chang Y, Das A, Liang P-Y, Lian X, Repina NA, et al.: Optogenetic-mediated cardiovascular differentiation and patterning of human pluripotent stem cells 2021; DOI: 10.1002/ggn2.202100011

Heng BC, Zhang X, Aubel D, Bai Y, Li X, Wei Y, et al.: Role of YAP/TAZ in Cell Lineage Fate Determination and Related Signaling Pathways. Front Cell Dev Biol 2020;8:1–23.

Hoang P, Kowalczewski A, Sun S, Winston TS, Archilla AM, Lemus SM, et al.: Engineering spatial-organized cardiac organoids for developmental toxicity testing. Stem Cell Reports 2021;16:1228–1244.

Hofbauer P, Jahnel SM, Papai N, Giesshammer M, Deyett A, Schmidt C, et al.: Cardioids reveal self-organizing principles of human cardiogenesis. Cell 2021;184:3299–3317.e22.

Hofer M, Lutolf MP: Engineering organoids. Nat Rev Mater 2021;6:402–420.

Kilian KA, Bugarija B, Lahn BT, Mrksich M: Geometric cues for directing the differentiation of mesenchymal stem cells. Proc Natl Acad Sci U S A 2010;107:4872–4877.

Kim J, Koo BK, Knoblich JA: Human organoids: model systems for human biology and medicine. Nat Rev Mol Cell Biol 2020;21:571–584.

Kolind K, Leong KW, Besenbacher F, Foss M: Guidance of stem cell fate on 2D patterned surfaces. Biomaterials 2012;33:6626–6633.

Lee J, Sutani A, Kaneko R, Takeuchi J, Sasano T, Kohda T, et al.: In vitro generation of functional murine heart organoids via FGF4 and extracellular matrix. Nat Commun 2020;11. DOI: 10.1038/s41467-020-18031-5

Lewis-Israeli YR, Wasserman AH, Gabalski MA, Volmert BD, Ming Y, Ball KA, et al.: Self-assembling human heart organoids for the modeling of cardiac development and congenital heart disease. Nat Commun 2021;12. DOI: 10.1038/s41467-021-25329-5

Lian X, Hsiao C, Wilson G, Zhu K, Hazeltine LB, Azarin SM, et al.: Robust cardiomyocyte differentiation from human pluripotent stem cells via temporal modulation of canonical Wnt signaling. Proc Natl Acad Sci 2012;109:E1848–E1857.

Lian X, Zhang J, Azarin SM, Zhu K, Hazeltine LB, Bao X, et al.: Directed cardiomyocyte differentiation from human pluripotent stem cells by modulating Wnt/β-catenin signaling under fully defined conditions. Nat Protoc 2013;8:162–175.

Loye AM, Kinser ER, Bensouda S, Shayan M, Davis R, Wang R, et al.: Regulation of Mesenchymal Stem Cell Differentiation by Nanopatterning of Bulk Metallic Glass. Sci Rep 2018;8:1–11.

Ma Z, Wang J, Loskill P, Huebsch N, Koo S, Svedlund FL, et al.: Self-organizing human cardiac microchambers mediated by geometric confinement. Nat Commun 2015;6. DOI: 10.1038/ncomms8413

Martyn I, Brivanlou AH, Siggia ED: A wave of WNT signaling balanced by secreted inhibitors controls primitive streak formation in micropattern colonies of human embryonic stem cells. Dev 2019;146. DOI:

10.1242/dev.172791
McKee C, Chaudhry GR: Advances and challenges in stem cell culture. Colloids Surfaces B Biointerfaces 2017;159:62–77.
Mills RJ, Titmarsh DM, Koenig X, Parker BL, Ryall JG, Quaife-Ryan GA, et al.: Functional screening in human cardiac organoids reveals a metabolic mechanism for cardiomyocyte cell cycle arrest. Proc Natl Acad Sci U S A 2017;114:E8372–E8381.
Minn KT, Dietmann S, Waye SE, Morris SA, Solnica-Krezel L: Gene expression dynamics underlying cell fate emergence in 2D micropatterned human embryonic stem cell gastruloids. Stem Cell Reports 2021;16:1210–1227.
Minn KT, Fu YC, He S, Dietmann S, George SC, Anastasio MA, et al.: High-resolution transcriptional and morphogenetic profiling of cells from micropatterned human esc gastruloid cultures. Elife 2020;9:1–34.
Morgani SM, Metzger JJ, Nichols J, Siggia ED, Hadjantonakis AK: Micropattern differentiation of mouse pluripotent stem cells recapitulates embryo regionalized cell fate patterning. Elife 2018;7:1–35.
Nelson CM, Gleghorn JP: Sculpting organs: Mechanical regulation of tissue development. Annu Rev Biomed Eng 2012;14:129–154.
Nemashkalo A, Ruzo A, Heemskerk I, Warmflash A: Morphogen and community effects determine cell fates in response to BMP4 signaling in human embryonic stem cells. Dev 2017;144:3042–3053.
Shukla A, Slater JH, Culver JC, Dickinson ME, West JL: Biomimetic Surface Patterning Promotes Mesenchymal Stem Cell Differentiation. ACS Appl Mater Interfaces 2016;8:21883–21892.
Simunovic M, Brivanlou AH: Embryoids, organoids and gastruloids: New approaches to understanding embryogenesis. Dev 2017;144:976–985.
Tang J, Peng R, Ding J: The regulation of stem cell differentiation by cell-cell contact on micropatterned material surfaces. Biomaterials 2010;31:2470–2476.
Tewary M, Ostblom J, Prochazka L, Zulueta-Coarasa T, Shakiba N, Fernandez-Gonzalez R, et al.: A stepwise model of reaction-diffusion and positional information governs self-organized human peri-gastrulation-like patterning. Dev 2017;144:4298–4312.
Virdi JK, Pethe P: Biomaterials Regulate Mechanosensors YAP/TAZ in Stem Cell Growth and Differentiation. Tissue Eng Regen Med 2021;18:199–215.
Wan LQ, Ronaldson K, Park M, Taylor G, Zhang Y, Gimble JM, et al.: Micropatterned mammalian cells exhibit phenotype-specific left-right asymmetry. Proc Natl Acad Sci U S A 2011;108:12295–12300.
Warmflash A, Sorre B, Etoc F, Siggia ED, Brivanlou AH: A method to recapitulate early embryonic spatial patterning in human embryonic stem cells. Nat Methods 2014;11:847–854.
Yang Y, Wang X, Huang TC, Hu X, Kawazoe N, Tsai WB, et al.: Regulation of mesenchymal stem cell functions by micro-nano hybrid patterned surfaces. J Mater Chem B 2018;6:5424–5434.
Yin X, Mead BE, Safaee H, Langer R, Karp JM, Levy O: Engineering Stem Cell Organoids. Cell Stem Cell 2016;18:25–38.
Zhang YS, Sevilla A, Wan LQ, Lemischka IR, Vunjak-Novakovic G: Patterning pluripotency in embryonic stem cells. Stem Cells 2013;31:1806–1815.

Figure Captions.

Figure 1. Template designs influenced tissue self-assembly of cardiac organoids. Cardiac organoids were generated using a series of (a) rectangular and (b) pentagram designs. Rectangles with the same total area were designed with different aspect ratio from 1:1 to 1:4 (R1 to R4). Pentagram geometries were varied by incrementally increasing the center pentagon area (P1 to P4), while adjusting the area of the triangular vertices to keep the area constant. Cardiac organoids were successfully generated in all (c) rectangular templates and (d) pentagram templates with positive expression of cardiomyocyte marker cardiac troponin T (green). Actin (red) was used to visualize the cell distribution across the entire organoids. (e) The rectangular geometries had a decreasing trend in organoid height with the increase of aspect ratio (*$p = 0.0002$). (f) The pentagram geometries showed that the P2 template, which is an ideal star polygon, generated the highest organoids (*$p < 0.0001$). Scale bars 200 μm.

Figure 2. Rectangular geometry influenced cardiac contractile functions. Cardiac functions were measured from video analysis of both fluorescent calcium flux and cardiac contraction motion for all the rectangular templates: (a) R1, (b) R2, (c) R3, (d) R4. As the aspect ratios of rectangular templates increased, (e) the beat rate decreased (*$p < 0.0001$), while (f) the area ratio increased (*$p < 0.0001$). With the increasing aspect ratio, (g) the maximum calcium flux was increased (*$p = 0.0028$) at a faster upstroke rate as indicated by (h) a shorter τ_0 (*$p < 0.0001$). Calcium decay rates (i) τ_{50} (*$p = 0.1152$) and (j) τ_{75} (*$p = 0.7358$) remained consistent at all the rectangular templates. When the aspect ratios of the rectangular templates were larger than 1:1 (not square template), the cardiac organoids showed significant higher (k) contraction velocities (*$p < 0.0001$) and (l) relaxation velocities (*$p < 0.0001$), indicating robust and strong contractile behaviors. Scale bars 500 μm.

Figure 3. Pentagram geometry can be tailored for optimal cardiac contractile functions. Cardiac functions were measured from video analysis of both fluorescent calcium flux and cardiac contraction motion for all the pentagram templates: (a) P1, (b) P2, (c) P3, (d) P4. As the center pentagon area was increased, though (e) no significant difference on the beat rate (*$p = 0.0142$), the cardiac organoids exhibited a significant decrease in (f) the area ratio (*$p < 0.0001$). In general, the cardiac organoids from P2 templates showed higher (g) max calcium flux (*$p = 0.0004$), longer calcium upstroke rate (h) τ_0 (*$p = 0.0124$), and longer calcium decay rate (i) τ_{50} (*$p = 0.0044$) and (j) τ_{75} (*$p = 0.0048$). (k) Contraction velocities (*$p < 0.0001$) and (l) relaxation velocities (*$p < 0.0001$) showed significantly greater contraction motion in the pentagram templates with smaller center pentagon area, with peak contraction occurring in the P2-templated organoids. Scale bars 500 μm.

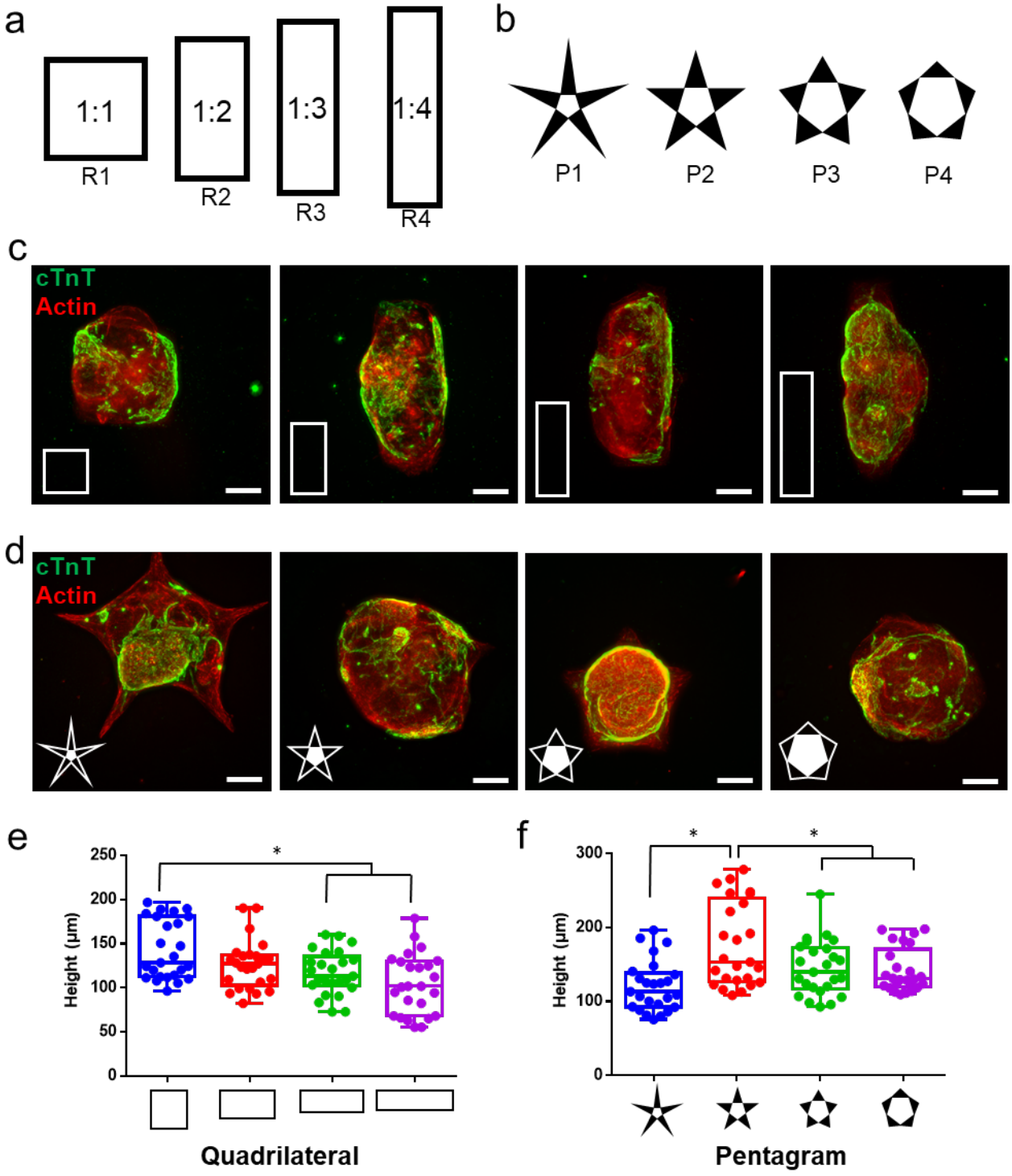
a
1:1
1:2
1:3
1:4
R1
R2
R3
R4
b
P1
P2
P3
P4
c
cTnT
Actin
d
cTnT
Actin
e
Height (μm)
250
200
150
100
50
0
*
Quadrilateral
f
Height (μm)
300
200
100
0
*
*
Pentagram

454

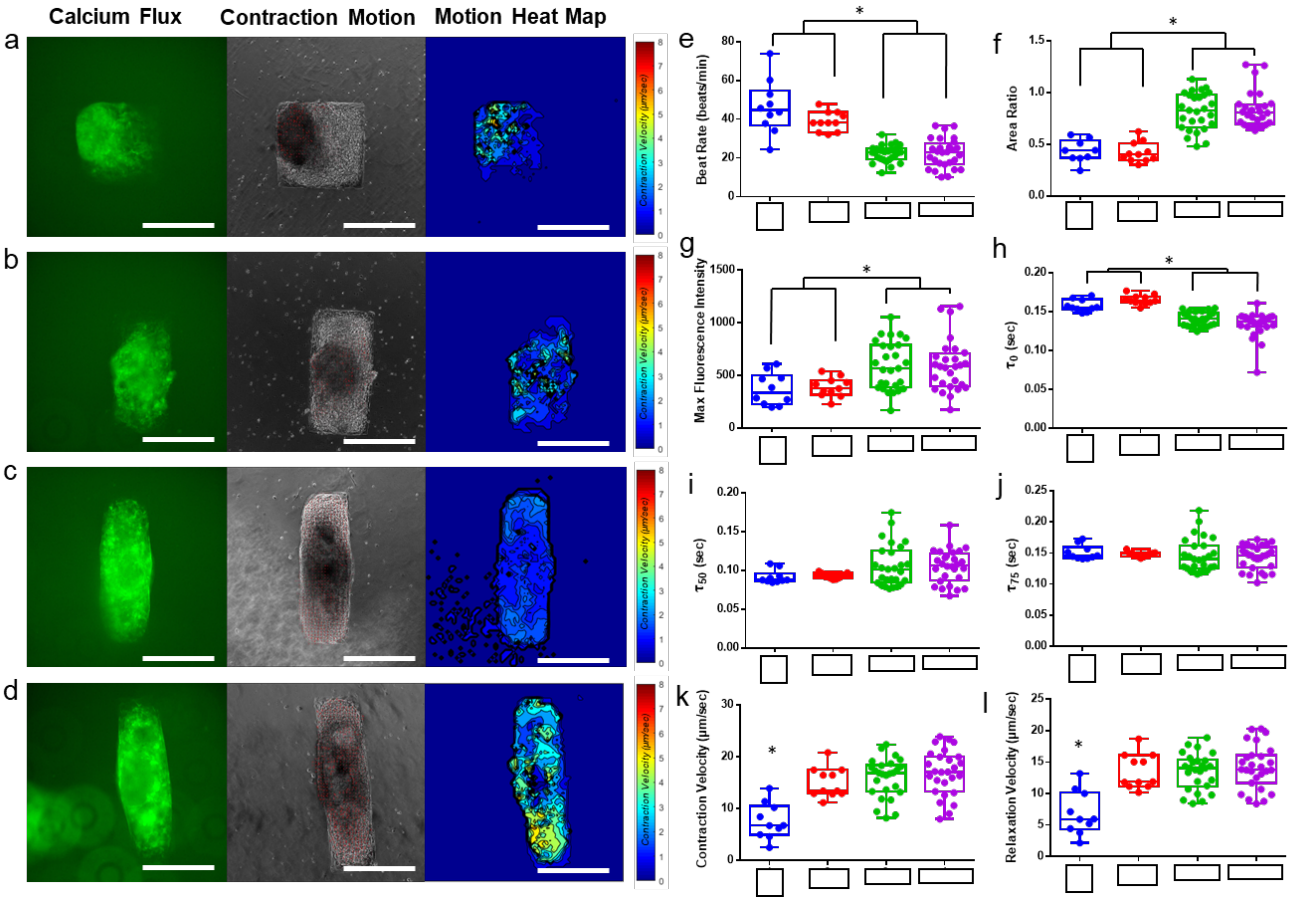
Calcium Flux
Contraction Motion
Motion Heat Map
a
b
c
d
Contraction Velocity (μm/sec)
e
Beat Rate (beats/min)
f
Area Ratio
g
Max Fluorescence Intensity
h
τ0 (sec)
i
τ50 (sec)
j
τ75 (sec)
k
Contraction Velocity (μm/sec)
l
Relaxation Velocity (μm/sec)
*

455

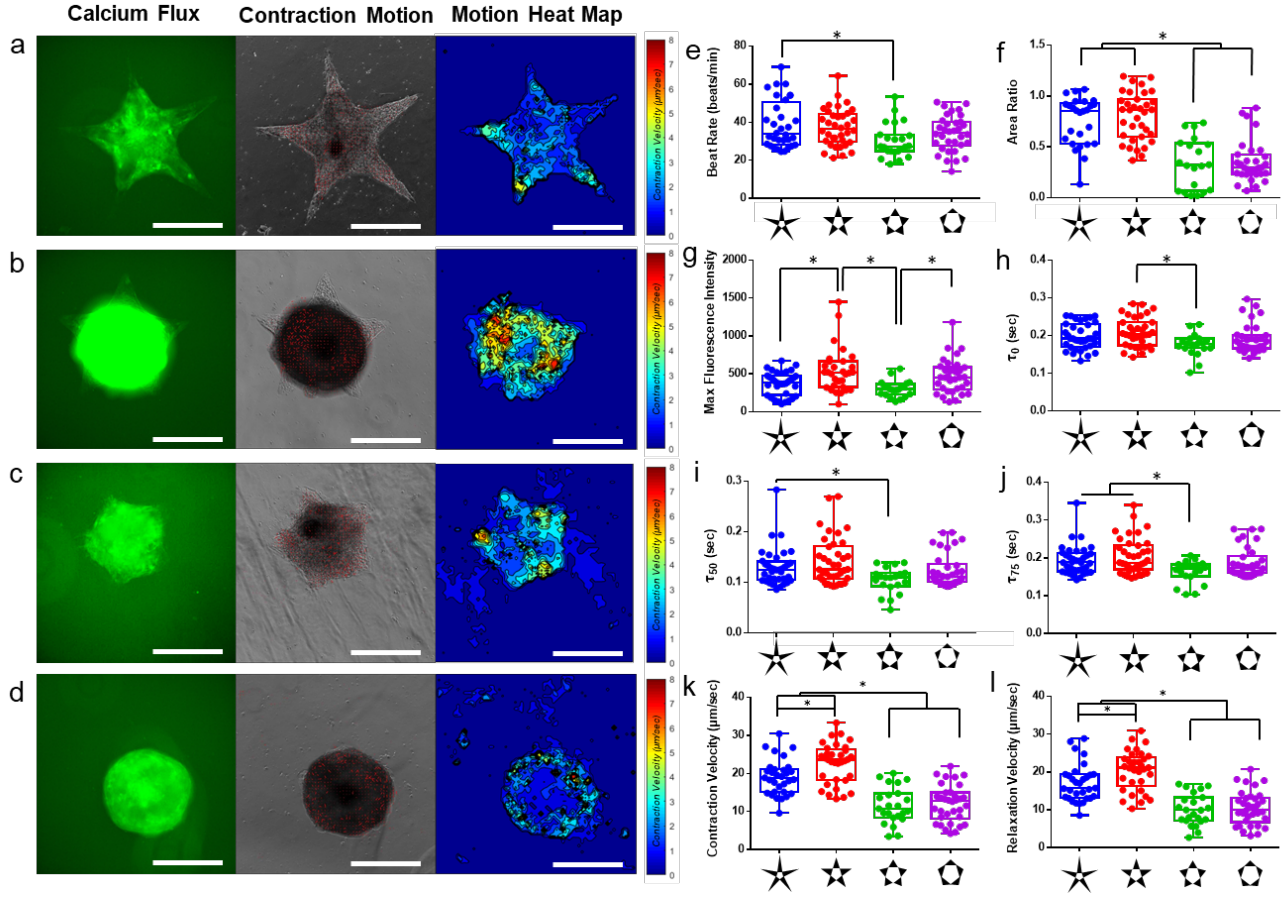
Calcium Flux
Contraction Motion
Motion Heat Map
a
b
c
d
e
f
g
h
i
j
k
l
Beat Rate (beats/min)
Area Ratio
Max Fluorescence Intensity
τ0 (sec)
τ50 (sec)
τ75 (sec)
Contraction Velocity (μm/sec)
Relaxation Velocity (μm/sec)
Contraction Velocity (μm/sec)

456